

PROPERTIES OF THE PROMPT OPTICAL COUNTERPART ARISING FROM THE COOLING OF
ELECTRONS IN GAMMA-RAY BURSTS

A.D. PANAITESCU AND W.T. VESTRAND

Intelligence and Space Research, MS D440, Los Alamos National Laboratory, Los Alamos, NM 87545, USA

Draft version September 27, 2022

ABSTRACT

This work extends a contemporaneous effort (Panaitescu & Vestrand 2022) to study the properties of the lower-energy counterpart synchrotron emission produced by the cooling of relativistic Gamma-Ray Burst (GRB) electrons through radiation (synchrotron and self-Compton) emission and adiabatic losses. We derive the major characteristics (pulse duration, lag-time after burst, brightness relative to the burst) of the Prompt Optical Counterpart (POC) accompanying GRBs and whose short timescale variability indicates a common origin with the burst.

Depending on the magnetic field life-time, duration of electron injection, and electron transit-time Δt_o from hard X-ray (GRB) to optical emitting energies, a (true) POC may appear during the GRB pulse (of duration δt_γ) or after (delayed OC). The signature of counterparts arising from the cooling of GRB electrons is that true POC pulses ($\Delta t_o < \delta t_\gamma$) last as long as the corresponding GRB pulse ($\delta t_o \simeq \delta t_\gamma$) while delayed OC pulses ($\Delta t_o > \delta t_\gamma$) last as long as the transit-time ($\delta t_o \simeq \Delta t_o$). If OC variability can be measured, then another signature for this OC mechanism is that the GRB variability is "passed" only to POCs but is lost for delayed OCs.

Within the GRB electron cooling model for counterparts, POCs should be on average dimmer than delayed ones (which is found to be consistent with the data), and harder GRB low-energy slopes β_{LE} should be associated more often with the dimmer POCs. The latter sets an observational bias against detecting POCs from (the cooling of electrons in) GRBs with a hard slope β_{LE} , making it more likely that the detected POCs of such bursts arise from another mechanism.

The range of low-energy slopes $\beta_{LE} \in [-1/2, 1/3]$ produced by electron cooling and the average burst brightness of 1 mJy (with 1 dex dispersion) imply that POCs of hard GRBs can be dimmer than $R = 20$ and difficult to detect by robotic telescopes (unless there is another mechanism that overshines the emission from cooling electrons) and that the POCs of soft GRBs can be brighter than $R = 10$, i.e. as bright as the Optical Flashes (OFs) seen for several bursts. All GRBs with OFs identified in this work have a hard low-energy slope β_{LE} , thus these OFs were not produced by the cooling of GRB electrons in a constant magnetic field.

In many cases, the lag-time Δt_o between GRB and POC is about 100 times longer than the cooling timescale of the GRB electrons, and that is the only new constraint on the GRB basic (non-temporal) model parameters that can be extracted from observations of POCs, with the POC-to-GRB brightness ratio constraining two temporal model parameters.

1. INTRODUCTION

The *prompt counterpart* is defined here as emission at an energy below the hard X-ray/ γ -ray of the main burst, and whose short variability timescale suggests a *common origin*. Simultaneity with the burst is not a requirement, as some prompt counterparts can appear during the burst (and are thus truly prompt), while other can appear after the burst. The latter will be called *delayed counterparts*, to avoid the oxymoron delayed prompt counterpart, and should not be confused with the afterglow, whose lack of short timescale variability indicates that it arises from a different mechanism. Given that a slowly-varying afterglow emission may exist even during the burst (e.g. GRB 050820A, whose OC was decomposed by Vestrand et al 2006 into a brighter afterglow-like emission and a dimmer component varying synchronously with the GRB), the identification of the prompt counterpart (as defined above) should be based on its short variability timescale and, when possible, on

its correlation with GRB pulses.

A short-lived *Prompt Optical Counterpart (POC)* emission has been detected during or after the prompt phase in many GRBs (e.g. sample listed by Kopac et al 2013) and could arise from these mechanisms:

i) the *reverse-shock* propagating in the GRB ejecta (Mészáros & Rees 1997, Panaitescu & Meszaros 1998) could produce a *delayed* bright POC occurring *after* the GRB pulse if its synchrotron emission peaks around the optical, as proposed for the *Optical Flash (OF)* of GRB 991023 by Mészáros & Rees (1999) and Sari & Piran (1999).

ii) optical emission arriving *before/during* the GRB pulse could be synchrotron emission from relativistic electrons, which is upscattered (synchrotron self-Compton) to produce the GRB emission (Papathanassiou & Mészáros 1996, Mészáros & Rees 1997), as proposed for the POC/OF of GRB 990123 by Panaitescu & Kumar (2007).

iii) *prompt/delayed* OCs could arise from the *pairs* (pro-

duced by GeV photons emitted during the GRB phase) that are accelerated by the forward-shock, as proposed for the OF of GRB 130427A by Vurm et al (2014), or which form in the shocked medium, as proposed for same OF by Panaitescu (2015).

Here, we study *only the synchrotron emission* from cooled GRB electrons as a mechanism for POCs, for electrons cooling through synchrotron (**SY**), inverse-Compton (**iC**) (as synchrotron self-Compton), or adiabatic (**AD**) losses. A POC dimmer than the burst results if the magnetic field lives shorter than the radiative cooling timescale t_{rad} of the typical GRB electron. If injection of the GRB electrons stops before t_{rad} but their cooling continues until they radiate SY emission in the optical, then the POC peak-flux will be the same as that of the burst (assuming a constant magnetic field). However, if the electron injection lasts longer than the electron transit-time from gamma to optical emission, then a bright POC can be produced.

We are interested in identifying temporal properties of POC resulting from the cooling of GRB electrons that can be used as identifiers of this mechanism for POCs, albeit there are few criteria to discriminate the POCs arising from the other three mechanisms above, most noteworthy being that

- i) POCs produced by the reverse-shock and pairs formed from the GeV prompt emission should and could, respectively, occur after the GRB and
- ii) POCs produced in the synchrotron self-Compton model for GRBs could occur before the prompt burst emission.

Table 1 lists the most often notations used here.

2. PROMPT COUNTERPART PROPERTIES

The analytical formalism for calculating the counterpart pulse light-curve $f_\epsilon(t)$ resulting from the cooling of GRB electrons is presented in a companion paper (Panaitescu & Vestrand 2022 - PV22). Those light-curves allow the calculation of the counterpart peak flux and its brightness relative to that of the GRB, quantified by the effective GRB-to-counterpart spectral slope $\beta_{e\gamma}$.

The counterpart peak epoch t_p depends on

- i) the time δt_ϵ that it takes electrons "to cool through" the observing energy, which is often equal to the time $t_{\gamma\epsilon}$ that it takes GRB electrons to migrate from γ -ray emitting energies to the energy ϵ at which the counterpart is observed,
 - ii) the lifetime t_B of the magnetic field and the duration t_I of electron injection,
- and, if the emitting surface is of uniform brightness,
- iii) the spread in photon arrival-time $t_{ang} = R/(2c\Gamma)$ (in the source frame, with R the source radius) across the ejecta surface of opening Γ^{-1} (the inverse of the source Lorentz factor) from which the observer receives a relativistically enhanced emission.

For pulses that are not too peaky or too stretched, the counterpart peak epoch t_p is also a good measure for the counterpart pulse duration δt_ϵ . Another quantity of interest is the time-lag Δt_ϵ between the GRB and the counterpart peak epochs, which depends on the transit-time

$t_{\gamma\epsilon}$ and the two timescales t_B and t_I for the magnetic field lifetime and electron injection, but is independent on the angular spreading timescale t_{ang} .

For ease of access, we reiterate here some of the analytical results for the above counterpart properties of interest.

If the pulse duration is set by radiative cooling (SY or iC through scatterings in the Thomson regime having a cooling power $P_{ic} \sim \gamma^2$), then the γ -to- ϵ electron transit-time $t_{\gamma\epsilon}^{(sy)}$ is

$$t_{\gamma\epsilon}^{(sy)} = \left(\frac{\epsilon}{E_\gamma}\right)^{-1/2} t_{sy,i} \quad (1)$$

Here, $t_{sy,i}$ is the SY-cooling timescale of the typical GRB γ_i electrons that radiate SY emission at the peak energy E_γ of the ϵF_ϵ GRB spectrum:

$$t_{sy}(\gamma_i) = \frac{\gamma_i m_e c^2}{P_{sy}(\gamma_i)} = \frac{8.10^8 s}{B^2 \gamma_i} \quad (2)$$

For iC-cooling through scatterings at the Thomson-Klein-Nishina transition, characterized by a cooling power $P_{ic} \sim \gamma^{2/3}$, the electron transit-time is

$$t_{\gamma\epsilon}^{(ic)} = t_{ic,i} \left[1 - \left(\frac{\epsilon}{E_\gamma}\right)^{1/6} \right] \quad (3)$$

where $t_{ic,i}$ is the iC-cooling timescale of the GRB γ_i -electrons.

For AD-dominated cooling and a power-law electron injection rate $R_i \sim t^y$

$$t_{\gamma\epsilon}^{(ad)} \simeq \left(\frac{\epsilon}{E_\gamma}\right)^{-3/4} \begin{cases} t_I & y < 1 \\ t_o & y > 1 \end{cases} \quad (4)$$

where t_o is the epoch (ejecta age) when electron injection began.

2.1. Prompt Counterpart Timing

Equations (A8) and (A20) of PV22 for radiative electron cooling show that the pulse-peak epoch is at $t_p = t_{\gamma\epsilon}$ if the electron injection lasts shorter than the transit-time ($t_I < t_{\gamma\epsilon}$) and for an exponent $n > 1$ (as for SY and iC cooling in the Thomson regime) of the electron cooling power $P(\gamma) \sim \gamma^n$; at $t_p \in [t_{\gamma\epsilon}, t_{\gamma\epsilon} + t_I]$ if $t_{\gamma\epsilon} < t_I$ for $n > 1$, and at $t_p = t_{\gamma\epsilon} + t_I$ for $n < 1$. Thus, $t_p = t_{\gamma\epsilon} + t_I$ is a good approximation for any ordering of $t_{\gamma\epsilon}$ and t_I , a result that can be extended to AD cooling with $t_{\gamma\epsilon} \equiv \hat{t}_{\gamma\epsilon}^{(ad)}$ for $y < 1$ and $t_{\gamma\epsilon} \equiv t_{\gamma\epsilon}^{(ad)}$ for $y > 1$ (but only if $t_{\gamma\epsilon}^{(ad)} > t_I$ in the latter case).

The above results are valid if the magnetic field lives $t_B > t_p$, i.e. if the electrons that yield the pulse peak cool to below the observing energy. Conversely, for a short-lived magnetic field with $t_B < t_p$, the pulse-peak epoch is set by t_B .

Thus, in general, the pulse peak-time is

$$t_p^{(\epsilon)} = \min\{t_I + t_{\gamma\epsilon}, t_B\} + t_{ang} \quad (5)$$

TABLE 1
GLOSSARY OF MORE FREQUENTLY USED NOTATIONS

Energies			
γ_i	typical energy of injected electrons	ϵ	observing photon energy
Spectral quantities			
β_{LE}	GRB low-energy slope (below E_γ)	$\beta_{o\gamma}$	optical-to-gamma effective spectral slope
E_γ	peak energy of GRB νF_ν spectrum	F_p	flux at E_γ
Electron timescales			
t_{ad}	AD cooling timescale	t_{rad}	radiative cooling timescale of γ_i electrons
t_{sy}	SY cooling timescale	t_{ic}	iC cooling timescale
$t_{sy,i}$	SY cooling timescale for the γ_i electrons	$t_{ic,i}$	iC cooling timescale for γ_i electrons
$t_{\gamma\epsilon}$	transit-time from GRB E_γ energy to ϵ	$t_{\gamma o}$	transit-time from GRB to optical (1 eV)
Other timescales			
t_B	magnetic field life-time	t_I	electron injection duration
δt_γ	duration of GRB pulse	δt_o	duration of POC pulse
t_p	pulse peak epoch	Δt_o	GRB-to-optical time-delay
t_{ang}	angular spread in photon arrival-time		

which, according to Equations (1), and (4), also provides a good estimate for the pulse duration δt_ϵ for all cooling processes except iC-cooling dominated by scatterings at the T-KN transition ($n = 2/3$), for which Equation (3) applies. That the peak-time t_p and pulse duration δt_ϵ are comparable is equivalent to a pulse rise and fall that are not too fast or too slow relative to the peak-time t_p .

From Equation (5), the **time-delay (lag)**

$$\Delta t_\epsilon = t_p^{(\epsilon)} - t_p^{(\gamma)} = \min\{t_{\gamma\epsilon} + t_I, t_B\} - \min\{t_{rad} + t_I, t_B\} \quad (6)$$

between the burst and the lower-energy pulse-peak epochs is independent of the angular time-spread t_{ang} . Here, t_{rad} is the radiative cooling timescale of the typical GRB γ_i electron: $t_{rad}^{-1} = t_{sy,i}^{-1} + t_{ic,i}^{-1}$.

Table 2 summarizes the temporal features expected for the GRB and lower-energy ϵ pulses resulting from the AD cooling or the radiative cooling with $n > 1$ of GRB electrons, for various orderings of the relevant timescales $t_{rad}, t_I, t_B, t_{\gamma\epsilon}$ and if the angular time-spread t_{ang} does not set the pulse duration.

For a short-lived magnetic field $t_B < t_I + t_{rad}$, pulses peak at t_B (cases 1-3), and the GRB-to-low-energy lag-time $\Delta t_\epsilon = 0$. For an electron injection duration satisfying $t_{\gamma\epsilon} < t_I < t_B$, pulses peak at t_I (case 4), yielding $\Delta t_\epsilon = t_{\gamma\epsilon} < t_I = \delta t_\gamma$. In all these cases, the counterpart is truly **Prompt**, defined by its peak occurring during the GRB pulse ($\Delta t_\epsilon < \delta t_\gamma$).

Delayed counterparts, defined by the pulse-peak appearing after the GRB pulse ($\Delta t_\epsilon > \delta t_\gamma$), occur when the electron injection lasts t_I shorter than the transit-time $t_{\gamma\epsilon}$ and when the magnetic field B is sufficiently long-lived $t_B > \max(t_I, t_{rad})$. If SY emission stops before the transit-time (i.e. $t_B < t_{\gamma\epsilon}$, cases 5-6), then the peak time-delay Δt_ϵ is the life-time t_B of the magnetic field. If SY emission is produced until after the transit-time (i.e. $t_B > t_{\gamma\epsilon}$, cases 7-8), then the peak time-delay Δt_ϵ is approximately the transit-time $t_{\gamma\epsilon}$ given in Equation (1) for SY-cooling, in Equations (4) for AD-cooling, and the $t_{\gamma\epsilon}^{(ic)}$ of Equation (3) for iC-cooling.

If the angular time-spread t_{ang} sets the pulse duration, then the duration of the GRB pulse δt_γ will be larger

than given in *Table 2* by at most a factor two. However, the angular time-spread t_{ang} does not affect the pulse-peak lag Δt_ϵ because the GRB and low-energy pulse-peak epochs are delayed by the same duration t_{ang} , thus the spherical curvature of the uniformly-emitting surface can change some delayed counterparts into prompt ones.

As shown in *Table 2*, prompt counterparts ($\Delta t_\epsilon < \delta t_\gamma$) should satisfy $\Delta t_\epsilon < \delta t_\epsilon \lesssim \delta t_\gamma$, i.e. *prompt counterpart and GRB pulse durations are comparable* and delayed counterparts ($\Delta t_\epsilon > \delta t_\gamma$) should satisfy $\delta t_\gamma < \delta t_\epsilon$ and $\Delta t_\epsilon \lesssim \delta t_\epsilon$, i.e. *a delayed counterpart lasts longer than the GRB pulse*.

Table 3 summarizes the temporal features of counterparts expected when the cooling of GRB electrons is dominated by iC scatterings at the T-KN transition, for which the cooling index is $n = 2/3$. This cooling process yields POCs pulses satisfying $t_p + \delta t_\epsilon = t_{ic,i} + t_I$ (Equation 3), which does not imply $t_p \simeq \delta t_\epsilon$, thus the counterpart pulse duration Δt_ϵ may not be comparable to its pulse peak-time $t_p^{(\epsilon)}$.

2.2. Prompt Counterpart Brightness (relative to GRB)

The pulse light-curves derived so far can be used to calculate the (peak-)flux at the counterpart pulse-peak and to convert the ratio of counterpart-to-GRB peak fluxes (at different peak-times, separated by Δt_o) to an effective counterpart/optical-to-GRB spectral slope

$$\beta_{\epsilon\gamma} = \frac{\log \frac{f_{pk}(\epsilon)}{f_{pk}(\gamma)}}{\log \frac{\epsilon}{E_\gamma}}, \quad \beta_{o\gamma} = -0.2 \log \frac{f_{pk}(1 \text{ eV})}{f_{pk}(100 \text{ keV})} \quad (7)$$

If the electron cooling is SY-dominated (or dominated by iC-scatterings in the Thomson regime and with an index $n = 2$), then the counterpart pulse light-curves given in equations (20)-(22) of PV22 lead to the OC-to-GRB slope

(SY/iC – Thomson)

TABLE 2

GRB and low-energy pulse properties FOR AN ELECTRON-COOLING DOMINATED BY **radiative losses** WITH $\mathbf{n} > 1$ OR BY **adiabatic losses**: *i)* PULSE-PEAK EPOCHS $t_p^{(\gamma)}$ AND $t_p^{(\epsilon)}$ *ii)* GRB-TO-LOW-ENERGY PEAK LAG $\Delta t_\epsilon \equiv t_p^{(\epsilon)} - t_p^{(\gamma)}$ (WHICH IS INDEPENDENT OF t_{ang}), *iii)* LOW-ENERGY-TO-GRB SLOPE $\beta_{e\gamma}$ FOR RADIATIVE-DOMINATED ELECTRON COOLING (DIMMEST COUNTERPART IS FOR $\beta_{e\gamma} = 1/3$, BRIGHTEST FOR $\beta_{e\gamma} = -(n-1)/2$; $\beta_{e\gamma} \sim 0$ MEANS THAT ANY VALUE BETWEEN THOSE EXTREMES IS POSSIBLE), FOR VARIOUS ORDERINGS OF THE RELEVANT TIMESCALES: COOLING t_{rad} OF THE GRB TYPICAL ELECTRONS, DURATION t_I OF ELECTRON INJECTION, LIFE-TIME t_B OF MAGNETIC FIELD, ELECTRON TRANSIT-TIME $t_{\gamma\epsilon} (> t_{rad})$ FROM GRB EMISSION TO OBSERVING ENERGY ϵ . COUNTERPARTS ARE "VERY PROMPT" IF $\Delta t_\epsilon \ll \delta t_\gamma$, **prompt** IF $\Delta t_\epsilon \leq \delta t_\gamma$, **delayed** IF $\Delta t_\epsilon > \delta t_\gamma$. COUNTERPART BRIGHTNESS IS RELATIVE TO THAT OF THE GRB, WITH AN "AVERAGE" COUNTERPART BRIGHTNESS CORRESPONDING TO $\beta_{e\gamma} = 0$, I.E. A COUNTERPART THAT IS AS BRIGHT AS THE BURST (E.G. MAGNITUDE $R = 16$ FOR A TYPICAL GRB PEAK-FLUX OF 1 MJY). THERE IS NO CLEAR CORRELATION BETWEEN THE COUNTERPART TYPE AND THE COUNTERPART-TO-GRB BRIGHTNESS RATIO. *Note:* FOR AD ELECTRON COOLING, t_B SETS THE DURATION OF SY EMISSION BUT HAS NO EFFECT ON ELECTRON COOLING. FURTHERMORE, BECAUSE THE AD-COOLING TIMESCALE IS THE CURRENT TIME, t_{rad} BECOMES t_I , THUS ONLY CASES SHOWN IN BOLD-FACE APPLY TO AD-COOLING. *Note:* THE ANGULAR TIME-SPREAD t_{ang} ASSOCIATED WITH THE EMISSION FROM A SPHERICALLY CURVED SURFACE INCREASES ALL TIMESCALES (INCLUDING $t_p^{(\gamma)}$ AND $t_p^{(\epsilon)}$) BY $\sim 50\%$, THUS THE TYPE OF OC DOES NOT CHANGE WHEN GOING FROM A BRIGHT-SPOT TO A SPHERICAL EMITTING SURFACE. HOWEVER, GIVEN THAT ONLY ELECTRON COOLING AND ANGULAR INTEGRATION INDUCE THE OBSERVED GRB PULSE-DURATION DECREASE WITH INCREASING ENERGY, THE GRB PULSES WHOSE DURATION δt_γ IS SET BY t_B OR t_I SHOULD BE INCONSISTENT WITH THAT TREND IF THE SY EMISSION AROSE FROM A BRIGHT-SPOT.

Case	$t_p^{(\gamma)}$ (= δt_γ)	$t_p^{(\epsilon)}$ (= δt_ϵ)	Δt_ϵ	Counterpart Type	$\beta_{e\gamma}$	Counterpart Brightness
1 $t_B < t_{rad}$	t_B	t_B	0	very prompt	1/3	dimmest
2 $t_{rad} < t_B < t_{\gamma\epsilon}, t_I$	t_B	t_B	0	very prompt	~ 0	any
3 $t_{rad} < t_{\gamma\epsilon} < t_B < t_I$	t_B	t_B	0	very prompt	$-(n-1)/2$	brightest
4 $t_{rad} < t_{\gamma\epsilon} < t_I < t_B$	t_I	$t_I + t_{\gamma\epsilon}$	$t_{\gamma\epsilon}$	prompt	$-(n-1)/2$	brightest
5 $t_I < t_{rad} < t_B < t_{\gamma\epsilon}$	t_{rad}	t_B	$\lesssim t_B$	delayed	> 0	dim
6 $t_{rad} < t_I < t_B < t_{\gamma\epsilon}$	t_I	t_B	$\lesssim t_B$	delayed	~ 0	any
7 $t_{rad} < t_I < t_{\gamma\epsilon} < t_B$	t_I	$t_{\gamma\epsilon}$	$\lesssim t_{\gamma\epsilon}$	delayed	< 0	bright
8 $t_I < t_{rad} < t_{\gamma\epsilon} < t_B$	t_{rad}	$t_{\gamma\epsilon}$	$\lesssim t_{\gamma\epsilon}$	delayed	0	average

TABLE 3

GRB and low-energy pulse properties FOR AN ELECTRON-COOLING DOMINATED BY **iC-scatterings at the T-KN transition** FOR WHICH $\mathbf{n} = 2/3$. BECAUSE THE TRANSIT-TIME $t_{\gamma\epsilon}$ IS SHORTER THAN THE IC-COOLING TIMESCALE t_{rad} OF THE TYPICAL GRB ELECTRON, THE ORDERING OF t_{rad} , t_I , AND t_B IS NOT RELEVANT. THERE IS NO CORRELATION BETWEEN THE COUNTERPART TYPE AND THE COUNTERPART-TO-GRB BRIGHTNESS RATIO. THE COUNTERPART-TO-GRB SLOPE IS LIKELY TO BE $\beta_{e\gamma} \gtrsim 0$, THUS THESE COUNTERPARTS ARISING FROM AN ELECTRON COOLING OF EXPONENT $n < 1$ ARE EXPECTED TO BE DIMMER, ON AVERAGE, THAN THOSE FOR AN ELECTRON-COOLING EXPONENT $n > 1$ (Table 2).

Case	$t_p^{(\gamma)}$	$t_p^{(\epsilon)}$	Δt_ϵ	CP Type	$\beta_{e\gamma}$	CP Brightness
1 $t_B < t_I, t_{\gamma\epsilon}$	t_B	t_B	0	very prompt	$< 1/3$	dimmer
2 $t_{\gamma\epsilon} < t_B < t_I$	t_B	t_B	0	very prompt	1/6	dim
3 $t_{\gamma\epsilon} < t_I, t_I + t_{\gamma\epsilon} < t_B$	t_I	$t_I + t_{\gamma\epsilon}$	$t_{\gamma\epsilon}$	prompt	0	average
4 $t_I < t_B < t_{\gamma\epsilon}$	t_I	t_B	$\lesssim t_B$	delayed	$< 1/3$	dimmer
5 $t_I, t_{\gamma\epsilon} < t_B < t_I + t_{\gamma\epsilon}$	t_I	t_B	$\lesssim t_B$	delayed	$< 1/6$	dimmer/average
6 $t_I < t_{\gamma\epsilon}, t_I + t_{\gamma\epsilon} < t_B$	t_I	$t_I + t_{\gamma\epsilon}$	$t_{\gamma\epsilon}$	delayed	0	average

$$\beta_{o\gamma} = \begin{cases} \frac{1}{3} & (1) \\ \frac{1}{3} - \frac{1}{3} \log \frac{t_B}{t_{sy,i}} & (2) \\ -\frac{1}{2} & (3) (4) \\ \frac{1}{3} - \frac{2}{15} \log \frac{t_B}{t_{sy,i}} & (5) \\ \frac{1}{3} - \frac{2}{15} \log \frac{t_B}{t_{sy,i}} - \frac{1}{15} \log \frac{t_I}{t_{sy,i}} & (6) \\ -\frac{1}{5} \log \frac{t_I}{t_{sy,i}} & (7) \\ 0 & (8) \end{cases} \quad (8)$$

This equation shows that both prompt and delayed OCs can be either dim and bright relative to the GRB, depending on the ratios $t_B/t_{sy,i}$ and $t_I/t_{sy,i}$, without any expected correlation between the POC type and the POC-to-GRB brightness ratio. Furthermore, for POCs with a slope $\beta_{o\gamma} \sim 0$ (i.e. between the extreme values $1/3$ and $-1/2$), a measured slope $\beta_{o\gamma}$ constrains the ratio $t_B/t_{sy,i}$, but the resulting constraint is unclear for delayed OCs.

When the electron cooling is AD-dominated, equations (B6) and (B8) of PV22 yield

for the cases listed in Table 2.

(AD : $\mathbf{R}_i \sim \mathbf{t}^{-y}, \mathbf{y} < 5/9$)

$$\beta_{o\gamma} = \begin{cases} \frac{1}{3} & (1) \\ \frac{1}{3} - \frac{4}{45} \log \frac{t_B}{t_I} & (5)(6) \\ 0 & (7)(8) \end{cases} \quad (9)$$

(AD : $5/9 < y < 1$)

$$\beta_{o\gamma} = \begin{cases} \frac{1}{3} - \frac{y-5/9}{5} \log \frac{t_B}{t_o} & (1) \\ \frac{1}{3} + \frac{1-y}{5} \log \frac{t_I}{t_o} - \frac{4}{45} \log \frac{t_B}{t_o} & (5)(6) (t_B < t_{\gamma\epsilon}) \\ \frac{3}{4} (1-y) - \frac{1-y}{5} \log \frac{t_B}{t_I} & (7)(8) (t_{\gamma\epsilon} < t_B < \hat{t}_{\gamma\epsilon}) \\ 0 & (7)(8) \end{cases} \quad (10)$$

(AD : $1 < y$)

$$\beta_{o\gamma} = \begin{cases} \frac{1}{3} - \frac{4}{45} \log \frac{t_B}{t_o} & (1)(5)(6) \\ 0 & (7)(8) \end{cases} \quad (11)$$

with the corresponding cases of *Table 2* indicated. Thus, if the electron injection rate does not decrease too fast ($y < 5/9$), a measured optical-to-GRB slope $\beta_{o\gamma}$ constrains the ratio t_B/t_I if $t_B > t_I$.

For an electron cooling dominated by iC-scatterings at the T-KN transition, when the cooling index is $n = 2/3$, equations (A18) and (A19) of PV22 lead to

(iC/T – KN)

$$\beta_{o\gamma} = \begin{cases} \frac{1}{3} + \frac{1}{5} \log \left(1 - \frac{t_B}{t_{ic}} \right) & (1) \\ \frac{1}{6} & (2) \\ 0 & (3) \\ \frac{1}{3} + \frac{1}{5} \log \left[\left(1 - \frac{t_B}{t_{ic}} \right) \left(1 - \frac{t_B - t_I}{t_{ic}} \right) \right] & (4) \\ \frac{1}{6} + \frac{1}{5} \log \left(1 - \frac{t_B - t_I}{t_{ic}} \right) & (5) \\ 0 & (6) \end{cases} \quad (12)$$

where t_{ic} is the iC-cooling timescale of the γ_i -electron and with the corresponding cases of *Table 3* identified. These results are valid for $t_I, t_B < t_{ic}$. Similar to $n > 1$ electron cooling, for POCs, a measured slope $\beta_{o\gamma}$ represents a constraint on the ratio t_B/t_{ic} .

2.3. GRB-to-Prompt Counterpart Lag-Time

From Equation (6), for a magnetic field with a life-time longer than the transit-time $t_B > t_{\gamma\epsilon}$, the pulse-peak lag-time $\Delta t_\epsilon = t_{\gamma\epsilon} - t_{rad} \lesssim t_{\gamma\epsilon}$ is close to the transit-time $t_{\gamma\epsilon}$ from GRB to the observing energy, given in Equations (1) for SY cooling, (4) for AD cooling, and (3) for iC cooling at the T-KN transition.

Corrections occur when the transit-time $t_{\gamma\epsilon}$ is sufficiently long that the electron-cooling departs from the cooling laws used above. As shown in *Appendix C* of PV22, if the cooling of the typical GRB γ_i -electron is initially SY-dominated ($t_{sy,i} < 1.5 t_o$), it becomes AD-dominated after a critical time t_{cr} , but the evolution of

the electron energy changes from the SY solution to 1/3-SY solution after a time equal to the initial ejecta age t_o . Thus, for $t_{\gamma\epsilon}^{(sy)} \gg t_o$, the correct transit-time $t_{\gamma\epsilon}^{(sy)}$ can be up to three times shorter than given in Equation (1).

If the cooling of the GRB γ_i -electron is initially AD-dominated ($t_{sy,i} < 1.5 t_o$), then cooling remains AD-dominated at all times, yet a change in the electron cooling occurs at the epoch \tilde{t} of equation (C12) of PV22, when the electron cooling switches from the AD-solution to the 1/3-SY cooling, leading to a more substantial correction for the transit-time $t_{\gamma\epsilon}^{(ad)}$ if $t_{\gamma\epsilon}^{(ad)} > \tilde{t}$. This is of relevance for an electron injection rate $R_i \sim t^{-y}$ with $y > 1$, when the pulse peak-epoch is set by passage of the lowest-energy electrons.

For an electron injection rate with $y < 1$, the pulse peak-epoch is set by passage of the highest-energy electrons, whose cooling begins at time t_I , thus the initial cooling regime is set by the parameter $2t_{sy,i}/3t_I = t_{sy,i}/t_{ad}(t_I)$, and with a corresponding $t_o \rightarrow t_I$ substitution in the definition of the switch-time \tilde{t} . The calculation of the correct transit-time is further complicated if the critical energy $\gamma_{cr}(t) \simeq (2/3)\gamma_i t_{sy,i}/(t + t_o)$, where the AD and SY-cooling timescales are equal, crosses the observing energy ϵ before the high-end energy ϵ_p of the SY spectrum from the cooling-tail. As shown in fig 3 of PV22, the cooling-tail peaks below γ_{cr} (but that peak is very shallow and broad) and the pulse-peak epoch corresponds to the time when the SY characteristic energy for the γ_{cr} -electrons crosses the observing energy ϵ :

$$t_{\gamma\epsilon}^{(cr)} = \frac{2}{3} \left(\frac{E_\gamma}{\epsilon} \right)^{1/2} t_{sy,i} = \frac{2}{3} t_{\gamma\epsilon}^{(sy)} \quad (13)$$

Putting together all above corrections, the lag-time between the GRB peak and the pulse peak-time at energy $\epsilon < E_\gamma$ is

$$(\text{AD} + \text{SY} : R_i \sim t^{-y}) \quad Z \equiv \frac{t_{sy,i}}{t_{ad}(t=0)}$$

$$\Delta t_\epsilon = \begin{cases} t_{\gamma\epsilon}^{(sy)} & Z \ll \left(\frac{\epsilon}{E_\gamma} \right)^{1/2} \\ \frac{1}{3} t_{\gamma\epsilon}^{(sy)} & \left(\frac{\epsilon}{E_\gamma} \right)^{1/2} \ll Z < 1 \\ \frac{1}{3} t_{\gamma\epsilon}^{(sy)} (y > 1) & 1 < Z \ll \left(\frac{E_\gamma}{\epsilon} \right)^{1/4} \\ t_{\gamma\epsilon}^{(ad)} (y > 1) & \left(\frac{E_\gamma}{\epsilon} \right)^{1/4} \ll Z \\ t_{\gamma\epsilon}^{(cr)} (y < 1) & 1 < Z < \frac{t_I}{t_o} \left(\frac{E_\gamma}{\epsilon} \right)^{1/2} \ll 1 + \frac{t_I}{t_{sy,i}} \\ \hat{t}_{\gamma\epsilon}^{(ad)} (y < 1) & \frac{t_I}{t_o} < Z, \left(\frac{E_\gamma}{\epsilon} \right)^{1/4} \ll 1 + \frac{t_{sy,i}}{3t_I} \\ \frac{1}{3} t_{\gamma\epsilon}^{(sy)} (y < 1) & 1 < Z < \frac{t_I}{t_o} \left(\frac{E_\gamma}{\epsilon} \right)^{1/2} \gg 3 \left(1 + \frac{t_I}{t_{sy,i}} \right) \\ \frac{1}{3} t_{\gamma\epsilon}^{(sy)} (y < 1) & \frac{t_I}{t_o} < Z, \left(\frac{E_\gamma}{\epsilon} \right)^{1/2} \gg \left(\frac{t_{sy,i}}{3t_I} \right)^2 + \frac{t_{sy,i}}{3t_I} + 6 \end{cases} \quad (14)$$

assuming that electron injection lasts longer than the initial AD cooling timescale ($t_I > t_o$). The above branches lack continuity whenever the result shown is asymptotic.

By identifying the GRB-to-1-keV transit-time with those cases above that set a lower-limit on the observing energy ϵ , one obtains the GRB-to-X-ray pulse-peak lag

$$\Delta t_x \simeq \begin{cases} t_{\gamma\epsilon}^{(sy)} = 10 E_{\gamma,5}^{1/2} t_{sy,i} & Z \ll 0.07 E_{\gamma,5}^{-1/2} \\ t_{\gamma\epsilon}^{(ad)} = 30 E_{\gamma,5}^{3/4} t_o \quad (y > 1) & Z \gg 6 E_{\gamma,5}^{1/4} \\ t_{\gamma\epsilon}^{(cr)} = 7 E_{\gamma,5}^{1/2} t_{sy,i} \quad (y < 1) & 1 < Z < \frac{t_I}{t_o}, \frac{t_I}{t_{sy,i}} \gg 10 E_{\gamma,5}^{1/2} \\ \hat{t}_{\gamma\epsilon}^{(ad)} = 3 E_{\gamma,5}^{1/4} t_I \quad (y < 1) & \frac{t_I}{t_o} < Z, \frac{t_{sy,i}}{t_I} \gg 3 E_{\gamma,5}^{1/4} \end{cases} \quad (15)$$

and those cases above that set an upper limit on ϵ should be identified with the GRB-to-POC pulse-peak lag

$$\Delta t_o = \frac{1}{3} t_{\gamma\epsilon}^{(sy)} \simeq 100 E_{\gamma,5}^{1/2} t_{sy,i} \equiv t_{\gamma o}^{(sy)} \quad (16)$$

Thus, for all cases, the pulse peak-lag is 1/3 of the SY transit-time $t_{\gamma\epsilon}^{(sy)}$ and

$$0.01 E_{\gamma,5}^{-1/2} \ll \frac{t_{sy,i}}{t_o, t_I} \ll 50 E_{\gamma,5}^{1/4} \quad (17)$$

is satisfied, with the ratio above being close to $t_{sy,i}/t_{ad}$, where $t_{ad} = t_o$ (initial age) for $y > 1$ (fast decreasing electron injection rate) and $t_{ad} = t_I$ (electron injection duration) for $y < 1$.

If the SY-cooling timescale $t_{sy,i}$ of the GRB electrons is smaller than the lower limit above, then electrons are still in the SY-cooling regime by the time when they radiate in the optical, thus the transit time $t_{\gamma\epsilon}^{(sy)}$ will be three times longer than in Equation (16). If $t_{sy,i}$ is longer than the higher limit above, then electrons are still in the AD-cooling regime when they reach optically-emitting energies. The large gap of five decades between optical and GRB energies implies that, for GRB SY-cooling times $t_{sy,i}$ ranging over almost four orders of magnitude, the electron cooling should be in the 1/3-SY cooling regime when the electron has cooled enough to radiate in the optical. Owing to its proximity to GRB energies, the peak-lag Δt_x to soft X-rays (1 keV) has a more complex dependence on the initial cooling timescales (Equation 15).

The above results did not include iC cooling. When electron-cooling is iC-dominated by scatterings in the Thomson regime, the electron cooling-tail has a falling spectrum $f_\epsilon \sim \epsilon^{-1/2}$ and, as discussed in *Appendix A1* of PV22, the POC pulse peaks at epoch $t_{\gamma\epsilon}$ when the lowest energy electrons radiate in the optical, thus the gamma-to-optical transit-time is:

$$\text{(iC - Thomson)} \quad t_{\gamma o}^{(ic)} = (10^5 E_{\gamma,5})^{1/2} t_{ic,i} \simeq \frac{t_{\gamma o}^{(sy)}}{Y} \quad (18)$$

with $Y > 1$ the Compton parameter of the γ_i electrons, and $t_{\gamma o}^{(sy)}$ the gamma-to-optical transit-time for SY-dominated electron cooling (Equation 16). This result is accurate if t_{ic} and Y are constant, which is true if the condition for the growth of a power-law cooling-tail

is satisfied. Otherwise, the Compton parameter above is an average during the electron cooling.

When electron-cooling is iC-dominated by scatterings at the T-KN transition, the cooling-tail has a rising spectrum $f_\epsilon \sim \epsilon^{1/6}$ and *Appendix A2* of PV22 shows that the POC pulse peaks when the high-energy end of the cooling-tail falls below the optical (due to electron cooling after the end of electron injection at t_I) at epoch

$$\text{(iC - TKN)} \quad t_{\gamma o}^{(ic)} \lesssim t_I + t_{ic,i} = t_I + \frac{t_{\gamma o}^{(sy)}}{300 E_{\gamma,5}^{1/2} Y} \quad (19)$$

Equations (16), (18), and (19) give the GRB-to-POC pulse-peak delay for either the emission from a bright-spot or a uniformly bright, spherically-curved surface because, in the latter case, all observer-frame timescales are stretched by the same angular spread in photon-arrival time t_{ang} , thus the difference between the pulse-peak epochs at two different observing energies should be unaffected by the time-spread t_{ang} .

Over the visible surface of angular opening Γ^{-1} , the photons emitted from the edge (at angle $\theta = \Gamma^{-1}$ relative to radial direction) arrive at observer later by a duration t_{ang} than the photons emitted directly toward the observer (at angle $\theta = 0$) and have an energy in observer-frame that is twice smaller. This softening of the received emission due to the curvature of the emitting surface will delay pulse peaks at lower energies, but the delay should be much less than t_{ang} because the reduction in the relativistic boost by a factor 2 across the Γ^{-1} region is raised to the third power in the received spectral flux (or flux density), thus the pulse-peak at a lower energy will occur well before t_{ang} after the peak at a higher energy.

Using Equation (16), the GRB-to-POC peak delay should be unaffected by the photon-energy and arrival-time spreads over the Γ^{-1} visible region if $t_{\gamma o}^{(sy)} \simeq 100 t_{sy,i} \gtrsim t_{ang}/\text{few}$, which leads to $t_{sy,i} > 10^{-3} t_o$ after using Equation (17). Thus, the result of Equation (16) provides a robust estimate of the GRB-to-POC peak-lag Δt_o for a sufficiently long-lived magnetic field ($t_B > \Delta t_o$) and if electron iC-cooling is not dominant. Otherwise, the peak-lag time is that given in Equations (18) and (19).

3. OBSERVATIONAL CONSTRAINTS ON MODEL PARAMETERS

The GRB model has five *basic* parameters: GRB ejecta Lorentz factor Γ , typical electron energy $\gamma_i m_e c^2$, magnetic field B , total number of injected electrons N_e (in the bright-spot or in the visible Γ^{-1} region), and source radius R , and two *temporal* parameters: the timescales of electron injection t_I and magnetic field t_B .

3.1. Basic Model Parameters

The five fundamental parameters ($\Gamma, B, N_e, \gamma_i, R$) determine the following observables:

(1) the *peak-energy of the GRB spectrum*

$$E_\gamma = \frac{2 \times 10^{-8}}{z+1} B \Gamma \gamma_i^2 \text{ (eV)} \quad (20)$$

thus a measurement of E_γ sets this constraint on the basic model parameters

$$B \Gamma \gamma_i^2 = 5 \times 10^{12} (z+1) E_{\gamma,5} \quad (21)$$

(2) the *GRB-pulse duration* given in Equation (5), with the transit-time t_{γ_e} being the radiative cooling timescale t_{rad} . After taking into account that

i) the angular spread timescale t_{ang} is negligible in the case of a bright-spot (of angular opening $\delta\theta \ll \Gamma^{-1}$ much less than that of the area of maximal relativistic Doppler boost),

ii) for the emission from uniform-brightness surface, the angular spread is $t_{ang} = R/(2c\Gamma) = t_{co}/2$ is 1/3 of the AD-cooling timescale,

iii) the AD-cooling timescale is $t_{ad} = 1.5 t_{co}$,

with t_{co} the comoving-frame epoch corresponding to the end of electron injection or the disappearance of the magnetic field, the duration of the GRB pulse can be written as

$$\delta t_\gamma = \begin{cases} \min\{t_I + t_{rad}(B; N_e, R), t_B\} & (\delta\theta \ll \Gamma^{-1} + Rad) \\ \min\{t_I + t_{rad}, t_B\} + t_{ang} & (\delta\theta = \Gamma^{-1} + Rad) \\ \min\{2.5 t_I, 1.5 t_B\} \simeq 2(t_{co} - t_o) \delta\theta \ll \Gamma^{-1} + AD & \\ \min\{3 t_I, 2 t_B\} \simeq 3(t_{co} - t_o) & (\delta\theta = \Gamma^{-1} + AD) \end{cases} \quad (22)$$

for either Radiative (SY and iC) or Adiabatic-dominated electron cooling. For SY-dominated cooling, the radiative cooling timescale is $t_{rad} \equiv t_{sy,i}$ (Equation 2); for iC-dominated cooling $t_{rad} \equiv t_{ic,i} = t_{sy,i}/Y$ depends also on the number of electrons N_e and source radius R because they determine the electron scattering optical depth $\tau_e \sim N_e/R^2$ and the Compton parameter $Y(\gamma_i, N_e, R) \sim \gamma_i^2 \tau_e \sim \gamma_i^2 N_e/R^2$.

From the first line of Equation (22), it can be inferred that the GRB-pulse duration δt_γ is equal to the cooling timescale t_{rad} of the typical GRB electrons for the emission from a bright-spot, for a radiative-dominated electron-cooling, and for cases 5 and 8 of Table 2. In these cases, the constraint derived from the measured GRB pulse duration $\delta t_\gamma^{(obs)} = (z+1)\delta t_\gamma/\Gamma$ is

(bright – spot $\delta\theta \ll \Gamma^{-1} + Rad$; case 5, 8 – Table 2) :

$$B^2 \Gamma \gamma_i (Y+1) = 8 \times 10^8 \frac{z+1}{\delta t_\gamma^{(obs)}} \quad (23)$$

For a uniform-brightness surface and $\min(t_I, t_B) < t_{ang}$, the GRB-pulse duration δt_γ (second line of Equation 22) is set by the angular timescale t_{ang} , thus a measured δt_γ implies

(unif – surface $\delta\theta = \Gamma^{-1} + Rad$ or AD – cooling) :

$$\frac{R}{\Gamma^2} = (1-6) \times 10^{10} \frac{\delta t_\gamma^{(obs)}}{z+1} \quad (24)$$

constraint which is also valid for the last two lines of Equation (22), corresponding to AD-dominated electron

cooling, if the comoving-frame source-age $t_{co} = R/c\Gamma$ is larger than the age t_o when electron injection began.

(3) the *average/peak SY flux* F_p at the GRB peak-energy E_γ

$$F_p = \frac{100 \text{ Jy}}{4\pi D_l^2/(z+1)} B \Gamma^3 N_e \min \left\{ 1, \frac{t_{rad}}{\min(t_I, t_B)} \right\} \quad (25)$$

where D_l is the luminosity distance. The last term above accounts for the cooling of electrons below the peak E_γ (of the ϵF_ϵ power-per-decade): for $t_{rad} < \min(t_I, t_B)$, only a fraction $t_{rad}/\min(t_I, t_B) < 1$ of the total injected electrons N_e radiate at E_γ ; and only a fraction $(Y+1)^{-1}$ is released as SY emission (that factor is ignored). The last term above exists only for a radiative electron cooling because the AD-cooling timescale is the current time which implies $t_{rad} = t_I$ (with t_B being irrelevant for electron cooling).

The constraint provided by a measurement of the GRB peak-flux is

$$B \Gamma^3 N_e = 10^{52} \frac{D_{l,28}^2}{z+1} \frac{F_p}{m \text{ Jy}} \max \left\{ 1, \frac{\min(t_I, t_B)}{t_{rad}(B, N_e)} \right\} \quad (26)$$

where $D_{l,28}$ is the luminosity distance in units of 10^{28} cm. Note that the GRB peak-flux F_p does not depend on the temporal parameters t_I, t_B only if $\min(t_I, t_B) < t_{rad}$, which corresponds to cases 1, 5, and 8 of Table 2, all cases of Table 3, or if the electron cooling is AD-dominated.

(4) the *GRB-to-POC peak delay* Δt_o **only** for cases 4, 7, and 8 of Table 2 and for cases 3 and 6 of Table 3, when Δt_o is equal to the gamma-to-optical transit-time $t_{\gamma o}$, which is proportional to the cooling-time $t_{rad}(B; N_e, R)$ of the typical GRB electron. This is true whether the emission arises from a bright-spot or from a uniformly-bright surface because, for the latter, the angular time-spread t_{ang} delays equally both pulse-peak epochs. Furthermore, for SY-, AD-, and $n = 2$ iC-dominated cooling, Equations (16) and (18) can be combined to obtain the observer-frame GRB-to-POC lag-time $\Delta t_o^{(obs)} = (z+1)\Delta t_o/\Gamma$

(case 4, 7, 8 – Table 2) :

$$\Delta t_o^{(obs)} \simeq 100 E_{\gamma,5}^{1/2} \frac{z+1}{\Gamma} \frac{t_{sy,i}}{Y+1} \quad (27)$$

leading to

$$B^2 \Gamma \gamma_i (Y+1) \simeq 10^{11} (z+1) \frac{E_{\gamma,5}^{1/2}}{\Delta t_o^{(obs)}} \quad (28)$$

(5) the *GRB-to-optical effective slope* $\beta_{o\gamma}$ between the peak fluxes of the GRB and POC pulses, in the cases indicated in Equations (8) – (12), by setting the cooling timescale t_{rad} of the typical GRB electron.

3.2. Radiative or Adiabatic Cooling ?

For the above cases (4, 7, and 8 of Table 2, 3 and 6 of Table 3) where the GRB-to-POC lag-time Δt_o provides a direct measurement (Equation 27) of the radiative timescale $t_{rad} = t_{sy,i}/(Y+1)$ of the γ_i -electrons, one

can identify the radiative regime of those electrons using the AD-cooling timescale determined from the GRB duration (Equation 22).

But first, for a bright-spot emission and radiatively-cooling GRB electrons (first line of Equation 22) and for case 8 of Table 2, the GRB pulse duration is equal to the electron radiative-cooling timescale, $\delta t_\gamma = t_{rad}$, thus

$$\frac{\Delta t_o^{(obs)}}{\delta t_\gamma^{(obs)}} = 100 E_{\gamma,5}^{1/2} \quad (29)$$

Such long-delayed OCs are not found among the ten POCs of Table 4. According to Table 2, delayed OCs with $\Delta t_o = t_{\gamma o}$ are expected to have an average or above average brightness. Then, the lack of long-delayed OCs could mean that radiatively-cooling electrons, a bright-spot emission, and $t_I < t_{rad} < t_B$ occur in less than 10% of POCs. However, if the cooling timescale t_{rad} of the GRB electrons is very short, then it would be difficult to identify the 10 ms GRB pulse corresponding to an POC peaking only 1 s after it.

For a uniform-brightness surface and radiatively-cooling GRB electrons (second line of Equation 22), the GRB pulse duration is larger than the angular timescale ($\delta t_\gamma \gtrsim t_{ang}$) and the condition for radiative electron-cooling ($t_{rad} < t_{ad} = 3 t_{ang}$) implies

$$\frac{\Delta t_o^{(obs)}}{\delta t_\gamma^{(obs)}} \lesssim 100 E_{\gamma,5}^{1/2} \frac{t_{rad}}{t_{ang}} < 300 E_{\gamma,5}^{1/2} \quad (30)$$

which is satisfied by all POCs of Table 4. Thus, all POCs identified here *could* be from radiatively cooling electrons (but that is not necessarily so).

For an AD-dominated cooling of the γ_i electrons at the end of the GRB pulse, the GRB pulse duration (given in the last two lines of Equation 22) is larger than the AD-cooling timescale: $\delta t_\gamma = (2-3) t_{co} = (1.3-2) t_{ad}$. As discussed in Appendix C of PV22 and shown by some cases in Equation (14), depending on the $t_{sy,i}/t_{ad}(t=0) > 1$ ratio, the cooling-law of electrons may become a 1/3-SY solution well before the AD-cooling electrons radiate in the optical, so that the gamma-to-optical transit-time $t_{\gamma o}$ and the GRB-to-POC time-lag Δt_o are set by the SY-cooling timescale $t_{sy,i}$ of the GRB γ_i electrons. In that case, the condition for AD-dominated electron cooling ($t_{rad}(\gamma_i) > t_{ad} = 1.5 t_{co}$) implies

$$\frac{\Delta t_o^{(obs)}}{\delta t_\gamma^{(obs)}} = 100 E_{\gamma,5}^{1/2} \frac{t_{rad}}{(4-5) t_{ang}} > (50-75) E_{\gamma,5}^{1/2} \quad (31)$$

Such long-delayed OCs are *not* found in Table 4, which strengthens the previous suggestion that GRB electrons are cooling radiatively in at least 90% of bursts, with the caveat that a long-delayed OC may be dimmer than indicated in Table 2 (cases 7 and 8 for AD-cooling), i.e. there could be an observational bias against detecting them.

It is important to note that the above assessments are restricted to those cases where the radiative cooling timescale t_{rad} of the typical GRB electron can be measured from the GRB-to-POC time-lag Δt_o (Equation 27) and where the AD timescale t_{ad} at the end of

the GRB pulse (which is either the disappearance of the magnetic field at t_B or the end of electron injection at t_I) can be constrained/determined from the duration δt_γ of the GRB pulse, using the second or the last two lines of Equation (22), respectively.

3.3. Temporal Model Parameters

The two temporal parameters t_I and t_B for the duration of electron injection and magnetic field life determine:

i) the GRB pulse duration $\delta t_\gamma = \min(t_I, t_B)$, as shown for several cases in Tables 2 and 3), *only if* the SY emission arises from a bright-spot and that the electron-cooling is radiative-dominated (first line of Equation 22). In these cases, the δt_γ provides a direct measurement of either t_B or t_I (but the source radius R remains unconstrained).

ii) and the GRB peak (or average) flux F_p *only if* $t_{rad} < \min(t_I, t_B)$ (cases 2-7 in Table 2). In these cases, the F_p constrains the ratio $t_{rad}/\min(t_I, t_B)$ (Equation 25).

iii) the POC brightness relative to the GRB, quantified by the effective POC-to-GRB slope $\beta_{o\gamma}$ (Equations 8–12), for cases 2, 5, 6, 7 in Table 2 and cases 1, 4, 5 in Table 3). In most of these cases, the $\beta_{o\gamma}$ constrains either t_{rad}/t_B or t_{rad}/t_I .

Additionally, the magnetic field life-time t_B sets the GRB-to-POC lag-time Δt_o for cases 5 and 6 in Table 2 and cases 4 and 5 in Table 3. In these cases, the Δt_o provides a direct measurement of t_B , but there is no overlap with a direct determination of t_B from the GRB pulse duration δt_γ that could lead to a test of this model.

Lastly, intermediate GRB low-energy slopes $\beta_{LE} \sim 0$ require field life-times t_B that are just above the cooling timescale t_{rad} of the typical GRB electrons and should exhibit a good $t_B - \beta_{LE}$ correlation if $t_B \in (1, 5)t_{rad}$, for radiative electron cooling (equation 30 of PV22), and if $t_B \in (5 t_o, 5 t_I)$, for AD cooling (Equation 50 PV22). These correspond to the very POC of case 2 in Table 2 and Table 3, for which the GRB-to-POC time-lag $\Delta t_o \sim 0$ does not constrain the electron cooling timescale t_{rad} .

For these intermediate GRB low-energy slopes $\beta_{LE} \sim 0$, the power-law low-energy spectrum is not fully developed. Numerical calculations of that low-energy spectrum and fits to it with the Band function can quantify the $t_B/t_{rad} - \beta_{LE}$ correlation and provide an observational constraint on the ratio t_B/t_{rad} .

Measurements of the GRB low-energy slope could also be included in the determination of model parameters by assuming that the SY spectrum below the GRB peak-energy E_γ is a perfect power-law of exponent β_{LE} , turning to a 1/3 slope below the minimal energy ε_m reached by electron cooling after a duration t_B , and by using POC measurements during the GRB pulse (these POCs are very prompt). For example, for SY-dominated electron cooling, Equation (1) leads to

$$\log \left(1 + \frac{t_B}{t_{sy,i}} \right) = 2.5 \frac{1 - 3\beta_{o\gamma}}{1 - 3\beta_{LE}} \quad (32)$$

which is consistent with the second line of Equation (8)

for $t_B \in (1, 300)t_{sy,i}$.

This result quantifies the $\beta_{LE} - t_B$ correlation of equation (20) in PV22 but includes POC measurements. Consequently, it does *not* represent a substitute for the correlation that would be inferred from GRB observations alone (as described above) and is, instead, only a refinement of the second line of Equation (8), which assumed a GRB low-energy slope $\beta_{LE} = -1/2$, and which is now set to the measured slope β_{LE} .

We note that, in the framework of POCs arising from the cooling of GRB electrons, the duration δt_o of a POC follows from the duration δt_γ of the GRB pulse and that of a delayed OC follows from the GRB-to-POC peak-delay Δt_o , thus the measured POC pulse duration δt_o does not provide a constraint on the model parameters; instead, it can only serve as a test of the POC origin in the cooling of GRB electrons.

Summarizing the above, we conclude that the GRB pulse duration δt_γ and GRB-to-optical time-lag Δt_o may constrain directly the model temporal parameters t_B and t_I , and the GRB low-energy slope β_{LE} and GRB-to-optical slope $\beta_{o\gamma}$ constrain the ratio of the temporal parameters to the electron cooling timescale t_{rad} . For the cases listed in Tables 2 and 3, the observables Δt_o and $\beta_{o\gamma}$ provide up to two constraints on the model temporal parameters, observable β_{LE} provides another constraint only in case 2 (either Table) and a semi-constraint for all other cases, and observable δt_γ yields another constraint in most cases but only if the GRB emission arises from bright-spots and if electron cooling is radiative dominated.

We note that the equality of the two temporal parameters, $t_B = t_I$ (in a model where the production of magnetic fields and the acceleration of relativistic particles are inter-dependent), selects cases shown in Tables 2 and 3 for which $t_p^{(\gamma)} = t_p^{(\epsilon)}$, i.e. only POCs. Thus, the existence of delayed OCs shows that the magnetic field lifetime t_B and the duration of electron injection t_I are not always strictly equal.

3.4. Constraints on Basic Model Parameters

In the final tally, observations provide up to six constraints: $E_\gamma; \delta t_\gamma, F_p, \Delta t_o, \beta_{o\gamma}; \beta_{LE}$ (first for basic parameters, next four for both basic and temporal parameters, last for temporal parameters) for seven model parameters: five basic ($\Gamma, \gamma_i, B, N_e, R$) and two temporal (t_B, t_I).

Even if one focused only on the conditions under which the temporal parameters t_B and t_I do *not* determine the GRB pulse duration δt_γ , the GRB peak-flux F_p , and the GRB-to-POC peak-delay Δt_o (i.e. only the emission from a bright-spot and case 8 of Table 2, or the emission from AD-cooling electrons), one would still have only four constraints (Equations 21, 24, 26, 28) for five model parameters. This system of four equations can be solved after choosing a free model parameter to parameterize the remaining four model parameters. Using the source

Lorentz factor Γ for that parameterization leads to

$$\gamma_i = 3 \times 10^4 \left(\frac{E_\gamma}{100 \text{ keV}} \right)^{1/2} \left[(z+1) \frac{\Delta t_o^{(obs)}/10s}{\Gamma/100} \right]^{1/3} \quad (33)$$

$$B = 50 \left[\frac{z+1}{(\Gamma/100)(\Delta t_o^{(obs)}/10s)^2} \right]^{1/3} (G) \quad (34)$$

for cases 4, 7, and 8 of Table 2 and for $Y < 1$, and

$$R \lesssim (1-6) \times 10^{15} \left(\frac{\Gamma}{100} \right)^2 \frac{\delta t_\gamma^{(obs)}}{10(z+1)s} (cm) \quad (35)$$

for the emission from a uniform surface ($\delta\theta = \Gamma^{-1}$) and radiatively-cooling electrons or for AD-dominated cooling.

Constraints from the X-ray (1-10 keV) counterpart cannot break the degeneracy among the five model parameters because, for counterparts arising from the cooling of GRB electrons in a constant magnetic field, the prompt X-ray counterpart pulse duration, peak flux, and peak delay after to GRB should follow from the corresponding POC features. Conversely, the prompt X-ray and optical counterpart temporal and spectral properties not being consistent with each other would either constrain the evolution of the magnetic field or would indicate that the two emissions arise from different mechanisms.

Thus, the full determination of the five model basic parameters requires the addition of another *strong* observational constraint. Below, we discuss some weaker constraints that are either inequalities or rely on assuming some parameters for the afterglow dynamics.

3.4.1. Semi-Constraints

From transparency to SY self-absorption. The condition that the optical is above the SY self-absorption frequency (so that the optical continuum is not a hard $\beta_o = 2$) can be used to set a low-limit on the Lorentz factor:

$$\Gamma > (16 - 63) \left[\frac{D_{l,28}^6 (F_p/mJy)^3}{(z+1)^4 \Delta t_o^{(obs)}/10s} \right]^{1/8} \quad (36)$$

with the lowest value for SY-dominated electron cooling and emission from a uniform surface and the highest value for AD-dominated electron cooling.

From afterglow dynamics. This constraint follows from the expectation that the GRB emission is produced before the interaction of the GRB ejecta with the ambient medium leads to the deceleration of the post-GRB ejecta. Given that the dynamics of decelerating relativistic blastwaves, i.e. their radius $R_{bw}(t)$ and Lorentz factor $\Gamma_{bw}(t)$, are set by their kinetic energy and by the density of the circumburst medium, Kumar et al (2007) obtain upper-limits on the radius R and lower-limits on the Lorentz factor Γ of the GRB source using the timing of the first afterglow measurements.

From escape of GeV photons. The escape of 10-100 GeV photons requires a sub-unitary optical-thickness to pair-formation on the MeV burst photons (e.g. Abdo et al 2009), thus Fermi/LAT measurements of the GeV emission accompanying a GRB may set a stringent lower-limit Γ_{min} on the source Lorentz factor, with the source whose radius R determined from the GRB-pulse duration, as in Equation (24). Evidently, this method provides an accurate lower-limit Γ_{min} only if the GRB and GeV emissions arise from the same source, i.e. if the GeV emission occurs during the burst (temporal consistency) and if the GeV measurements lie on the extrapolation of the burst MeV spectrum above the peak-energy E_γ or have a spectral energy distribution consistent with that of the burst (spectral consistency).

4. DISCUSSION

4.1. Temporal Correlations between GRB and POC

By comparing the GRB-to-POC pulse-peak delay/lag Δt_o with the GRB pulse duration δt_γ , one can identify two types of POCs. *Prompt* POCs, defined by $\Delta t_o < \delta t_\gamma$ (i.e. POC pulse-peak occurs *during* the GRB pulse), arise when the pulse-peak epochs (or pulse durations) given in Equation (5) are both determined either by the duration of electron injection t_I or by the life-time t_B of the magnetic field. *Delayed* POCs, defined by $\Delta t_o > \delta t_\gamma$ (i.e. POC pulse-peak occurs *after* the GRB pulse) occur whenever the two pulse durations are determined by different factors that introduce different timescales.

The GRB and POC temporal features of *Tables 2 and 3* refer to the case when the spread t_{ang} in the photon arrival-time over the curved emitting surface does not set the pulse duration. If the electron cooling is dominated by a radiative process (i.e. $t_{sy,i}, t_{ic,i} < t_{ad} = 3t_{ang}$), that assumption is correct only if the emitting region is a bright spot of angular extent less than the Γ^{-1} region (moving toward the observer) of maximal Doppler boost. The same assumption is correct if the electron cooling is dominated by AD losses because, in that case, the comoving-frame angular timescale t_{ang} is less than the comoving-frame current age, which is comparable to the dominant timescale appearing in Equation (5) for the pulse-peak epoch and pulse duration.

For a radiative electron cooling ($t_{rad} < t_{ad}$) and an uniformly-emitting surface, the peak epochs and pulse durations are increased by the angular time-spread t_{ang} , but the pulse-peak lag-time Δt_o (Equation 6) remains unchanged. Consequently, including the angular time-spread t_{ang} in the peak-epoch and in the pulse duration will change some t_{ang} -free delayed OCs with $\Delta t_o > \delta t_\gamma$ into t_{ang} -included POCs with $\Delta t_o < \delta t_\gamma$, as the GRB pulse duration is increased.

With that limitation for the identification of POC types, one can search for correlations between the temporal/spectral properties of GRBs/POCs for these two types of POCs.

Figure 1, showing the OCs listed in **Table 4**, illustrates the temporal *correlation between POC type and*

optical-to-GRB pulse duration ratio $\delta t_o/\delta t_\gamma$ discussed in §2.1, which can be summarized as

$$\begin{cases} \text{prompt OC} : \Delta t_o < \delta t_o \simeq \delta t_\gamma \\ \text{delayed OC} : \delta t_\gamma < \delta t_o \simeq \Delta t_o \end{cases} \quad (37)$$

That the POCs shown in **Figure 1** display the above features derived from $t_p \simeq \delta t_o$ indicates that their electron cooling is not dominated by iC scatterings at the T-KN transition ($n < 1$).

For the brightest OCs, robotic telescopes may measure the OC variability associated with the GRB pulse variability. If the latter arises from (large-scale) fluctuations in the magnetic field, then the GRB and optical flux should fluctuate synchronously. However, such fluctuations should be easier to evidence in the OC only around its peak time, thus there will be a bias in detecting temporally-correlated GRB and OC fluctuations mostly in prompt OCs.

Figure 2 illustrates the diversity of POCs (from a truly prompt to a delayed OC) that is obtained by adjusting temporal factors (here, the duration t_I of electron injection) that determine the GRB pulse duration. **Figure 2** also shows that GRB fluctuations (here, resulting from a variable electron injection rate R_i) will "survive" electron cooling (in the sense that they will be displayed by a variable POC light-curve) if the injection rate variability timescale (which sets the GRB variability timescale δt_γ) is longer than the GRB-to-OC transit-time $t_{\gamma o}$ (which sets the GRB-to-optical pulse peak lag Δt_o for a full electron cooling), otherwise the cooled electrons of consecutive injection episodes reach optically-emitting energies in short succession, separated by a time-interval $\delta t_\gamma < t_{\gamma o}$, and integration over the curved emitting surface and over the synchrotron function will wipe-out any OC variability of timescale δt_γ .

Thus, electron cooling allows the "propagation" of the GRB variability to the OC only if $\Delta t_o < \delta t_\gamma$, i.e. only for POCs.

4.2. Spectral Correlations between GRB and POC

For a constant magnetic field, the electron cooling (through any process) yields an effective optical-to-GRB slope harder than the GRB low-energy slope, $\beta_{o\gamma} \geq \beta_{LE}$, with the equality resulting if either electrons do not cool significantly during the magnetic field life-time t_B , leading to $\beta_{LE} = \beta_{o\gamma} = \beta_o = 1/3$ with β_o being the optical continuum slope, or if electrons cool below optical during $\min(t_I, t_B)$, leading to $\beta_{LE} = \beta_{o\gamma} = \beta_o = -(n-1)/2$. If either the magnetic field life-time or electron injection duration satisfy $t_{rad} < t_B, t_I < t_{\gamma o}$, then the SY emission integrated spectrum peaks between optical and γ -rays and $\beta_{o\gamma} > \beta_{LE} - (n-1)/2$ ($\beta_o = 1/3$ or $\beta_o = -(n-1)/2$).

For a minimal electron cooling ($t_B < t_{rad}, \beta_{LE} = 1/3$), one expects *i*) a very POC (case 1 in *Tables 2 and 3*) because the magnetic field life-time sets the pulse duration and peak-epoch at any energy, and *ii*) an POC dimmer than the GRB by a factor $(E_\gamma/1eV)^{1/3} \simeq 40$ or about 4 magnitudes. For a typical GRB average flux of 1 mJy, the POC should be of magnitude $R = 20$; for a bright GRB

TABLE 4

Temporal and spectral properties of some GRBs with Prompt Optical Counterparts. THE BURST PULSE NUMBER AND THE GRB INSTRUMENT ARE INDICATED (KW=KONUS-WIND). THE $t_p^{(\gamma)}$ IS THE GRB PEAK EPOCH MEASURED FROM TRIGGER (NOT FROM THE BEGINNING OF THE PULSE) AND IS OF NO USE, BUT IS LISTED HERE FOR IDENTIFYING THE GRB PULSE.

GRB PULSE DURATION δt_γ AND OPTICAL PULSE DURATION δt_o ARE THE WIDTH AT HALF-MAXIMUM READ FROM THE LIGHT-CURVES FOUND IN REFERENCES; Δt_o IS THE GRB-TO-POC PEAK DELAY/LAG-TIME; THEIR UNCERTAINTIES ARE 10-20%. THE GRB LOW-ENERGY SLOPE β_{LE} IS TAKEN FROM GCN CIRCULARS AND HAS AN UNCERTAINTY OF AT LEAST 0.1. THE EFFECTIVE SLOPE $\beta_{o\gamma}$ BETWEEN THE OPTICAL AND γ PULSE-PEAK FLUXES (SEPARATED BY Δt_o) WAS CALCULATED FROM PEAK FLUXES FOUND IN REFERENCE, AND HAS AN UNCERTAINTIES LESS THAN 0.1. **Prompt OCs** ARE DEFINED BY $\Delta t_o < \delta t_\gamma$ (OPTICAL PEAK OCCURRING DURING THE GRB PULSE), **Delayed OCs** ARE DEFINED BY $\Delta t_o > \delta t_\gamma$ (OPTICAL PEAK OCCURRING AFTER THE GRB PULSE). ONE EXPECTS THAT $\delta t_o \simeq \delta t_\gamma$ FOR POCs AND $\delta t_o \simeq \Delta t_o$ FOR DELAYED OCs, FOR EITHER TYPE, IT IS ALSO EXPECTED THAT $\beta_{LE} \leq \beta_{o\gamma}$, WITH THE EQUALITY TAKING PLACE FOR $\beta_{LE} = \beta_{o\gamma} = 1/3$ OR $-1/2$.

Optical Flashes ARE COUNTERPARTS WITH AN OPTICAL EMISSION BRIGHTER THAN THE EXPECTATION FOR THE COOLED GRB ELECTRONS (IN A CONSTANT MAGNETIC FIELD) AND SATISFY $\beta_{LE} > \beta_{o\gamma}$. AS SHOWN IN FIGURE 1, MOST OFS DO NOT DISPLAY THE ABOVE TEMPORAL CORRELATIONS EXPECTED FOR POCs (IF $\Delta t_o < \delta t_\gamma$ THEN $\delta t_o \simeq \delta t_\gamma$) OR FOR DELAYED POCs (IF $\Delta t_o > \delta t_\gamma$ THEN $\delta t_o \simeq \Delta t_o$). EVIDENTLY, THERE IS AN OBSERVATIONAL BIAS IN FAVOR OF DETECTING OFS USING ROBOTIC TELESCOPES THAN FOLLOWING UP DIM POCs WITH $\beta_{o\gamma} = 1/3$, WHICH IMPLIES THAT THE MEASURED SLOPES $\beta_{o\gamma}$ ARE SOMETIMES SOFTER THAN EXPECTED FOR THE COOLING OF GRB ELECTRONS.

GRB	Pulse	$t_p^{(\gamma)}$							Reference
	(Cooling) Prompt OC	(s)	$\delta t_\gamma \simeq \delta t_o > \Delta t_o$			$\beta_{LE} \leq \beta_{o\gamma}$			
060526	2 (BAT)	255	30	35	10	-0.5	0.0	Thone 2010, Kopac 2013	
061121	3 (KW)	72	8	10	5	-0.3	0.1	Page 2007	
110205	3 (BAT)	210	20	15	5	-0.5	0.2	Cucchiara 2011, Gendre 2012	
120711	2 (IBIS)	90	25	30	20	-0.4	-0.5	Martin-Carrillo 2014	
130925	2 (KW)	2650	280	300	290	-0.4	0.0	Greiner 2014	
	(Cooling) Delayed OC		$\delta t_\gamma < \delta t_o \simeq \Delta t_o$			$\beta_{LE} \leq \beta_{o\gamma}$			
041219	3 (BAT)	430	15	30	35	-0.7	-0.4	Vestrand 2005, Blake 2005	
060904B	1 (BAT)	2	4	70	50	-0.5	0.1	Klotz 2008, Kopac 2013	
091024	1 (KW)	5	15	450	420	-0.5	-0.5	Gruber 2011	
091024	5 (KW)	930	130	1400	1800	-0.4	-0.4	Virgili 2013	
111209	3 (KW)	2000	350	500	450	-0.3	0.0	Stratta 2013	
	Optical Flashes		δt_γ	δt_o	Δt_o	$\beta_{LE} > \beta_{o\gamma}$			
990123	1 (BATSE)	25	10	40?	22?	0.4	-0.6	Akerlof 1999	
990123	2 (BATSE)	37	10	40?	10?	0.0	-0.6	Corsi 2005	
080319B	1 (BAT)	18	22	25	2	0.15	-0.7	Racusin 2008, Wozniak 2009	
121217	2 (GBM)	730	8	45	10-20	0.4	0.1	Elliott 2014	
130427A	2 (GBM)	8	6	< 12	~ 5	0.0	-0.5	Ackermann 2014, Vestrand 2014	
160625B	1 (KW,GBM)	195	20	20	10-20	0.2	-0.4	Karpov 2017, Ravasio 2018	

with an average flux of 10 mJy, one gets $R = 18$. Even for the latter case, the POC, occurring during the burst, is too dim to be monitored by robotic telescopes at such early times, thus there will be a bias against following-up POCs arising from the cooling of electrons in GRBs with a hard low-energy slope. When such POCs are detected (as for GRB 990123 – Table 4), it is more likely that that optical emission arises from another mechanism, a possibility that can be tested (§4.3).

If electrons cool well below gamma-rays ($t_B > t_{rad}$, $\beta_{LE} = -1/2$ for SY-dominated electron cooling), the POC may be either prompt or delayed, and the POC may be brighter than the GRB by a factor up to $(E_\gamma/1eV)^{1/2} \simeq 300$, or about 6 magnitudes. For an average GRB flux of 1 mJy, the maximal POC brightness is $R = 10$, while brighter bursts, with an average flux of 10 mJy, could yield an POC of $R = 7.5$, thus the cooling of GRB electrons may account for the OFs of bright bursts such as GRB 090123, 080319B, or 130427A (Table 4).

The above considerations suggest a correlation between:

i) POC type and GRB low-energy slope β_{LE} , induced by GRBs with a short magnetic field life-time $t_B < t_{rad}$:

harder slopes β_{LE} should be associated more often with POCs than with delayed OCs. All POCs in Table 4 have soft low-energy slopes $\beta_{LE} \in (-0.5, -0.3)$ in a narrow range, thus this correlation cannot be tested with the POCs identified here.

ii) optical-to-GRB $\beta_{o\gamma}$ and GRB low-energy β_{LE} slopes, induced by their dependence on the magnetic field life-time t_B , which can be quantified using equations (30), (34), (48)–(50) of PV22 for the slope β_{LE} and Equations (8)–(12) for the effective slope $\beta_{o\gamma}$. For SY-dominated electron cooling, the slope $\beta_{o\gamma}$ on the 2nd and 4th branches of Equation (8) show that a magnetic field life-time $t_B \in (0, 10) t_{sy,i}$ yields correlated slopes $\beta_{o\gamma} \in (0, 1/3)$ and $\beta_{LE} \in (-1/2, 1/3)$, while for $t_B > 10 t_{sy,i}$, the resulting range of slopes $\beta_{o\gamma} \in (-1/2, 0)$ is uncorrelated with the only slope $\beta_{LE} = -1/2$.

In general, this correlation can be written as a condition: $\beta_{LE} \geq \beta_{o\gamma}$, meaning that GRBs with harder low-energy slopes are associated more often with dimmer POCs. If the POC emission from cooling GRB electrons is not overshadowed by another mechanism, then the observational bias against following such dimmer POCs will lead to a paucity of GRBs with hard low-energy slopes

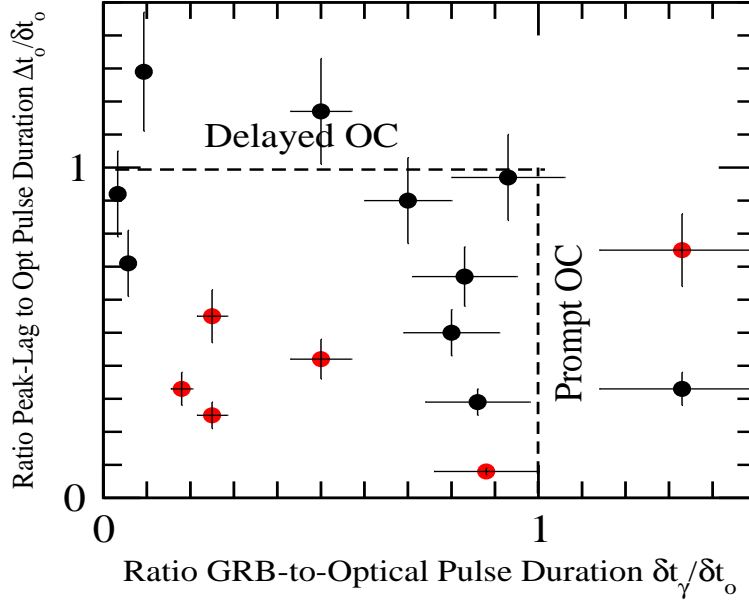


FIG. 1.— Comparison between the temporal properties (GRB-to-OC pulse-peak lag-time Δt_o , optical pulse duration δt_o , GRB pulse duration δt_γ) of the GRBs and POCs of Table 4 and the expectations for the POCs arising from cooling of the GRB electrons (Equation 37), shown with dashed lines. Given that two of these quantities should be equal, the diversity of POCs can be captured by plotting duration ratios with same denominator for both axes. Then, we expect prompt OCs to be spread around a vertical segment of unitary length at $\delta t_\gamma / \delta t_o = 1$ on the abscissa and delayed OCs to cluster around a horizontal segment of length unity at $\Delta t_o / \delta t_o = 1$ on the ordinate. Black symbols are for POCs whose optical-to-GRB effective spectral slope $\beta_{o\gamma}$ is consistent with the GRB low-energy slope β_{LE} (meaning that $\beta_{LE} \leq \beta_{o\gamma}$) if POCs were produced by the cooling of GRB electrons in a constant magnetic field. The error bars correspond to a plausible uncertainty σ of 10% for our (eye-balling) estimation of durations. Half of all such POCs are consistent with the temporal expectations (dashed lines) arising from the cooling of GRB electrons. Within 2σ , nearly all such POCs are consistent with those expectations. Red symbols are for POCs with peak brightness (relative to the GRB's) exceeding the expectations for electrons cooling in a constant magnetic field, i.e. for OFs with $\beta_{LE} > \beta_{o\gamma}$. Two-thirds of OFs are not consistent (farther than 2σ) with the expectations for the GRB electron cooling which, together with their excessive brightness, suggests that OFs arise from a different mechanism.

and POCs, which accounts for softness of the GRBs with the POCs listed in Table 4.

iii) POC type and POC-to-GRB relative brightness (quantified by the effective slope $\beta_{o\gamma}$), with POCs being dimmer on average than delayed ones. This correlation is supported by the POCs of Table 4, with the average slope $\beta_{o\gamma}$ of the former being harder than for the latter.

Optical extinction and reddening by dust in the host galaxy. Correlations involving the POC brightness may be weakened by the hard-to-determine accurately dust-extinction in the host galaxy, with an extinction $A_{V,h}$ in the host galaxy frame reducing the POC brightness by about $(1+z)A_{V,h}$ magnitudes (for a linear reddening curve). Thus, dust-extinction hardens the slope $\beta_{o\gamma}$ by $\delta\beta_{o\gamma} = 0.4(z+1)A_{V,h}/5$. For $A_{V,h} = 1$ mag and a redshift $z = 2$, the resulting hardening $\delta\beta_{o\gamma} = 1/4$ is about one-third of the entire expected range $\beta_{o\gamma} \in (-1/2, 1/3)$.

Furthermore, dust extinction is accompanied by a softening of the optical continuum slope β_o by $\delta\beta_o = -0.4(z+1)A_{V,h}$, i.e. $\delta\beta_o = -1.2$ for $z = 2$ and $A_{V,h} = 1$ mag, thus a hard intrinsic optical slope $\beta_o^{(intr)} = 1/3$ (expected for a magnetic field that lives shorter than the GRB-to-POC transit-time, $t_B < t_{\gamma o}$) could become a softer measured slope $\beta_o^{(dust)} \simeq -1$.

4.3. Identification of POCs from Cooling of GRB Electrons

Thus, the temporal correlation between POC type and the optical-to-GRB pulse duration ratio $\delta t_o / \delta t_\gamma$ and the spectral condition $\beta_{o\gamma} > \beta_{LE}$ between the optical-to-GRB effective slope and the GRB low-energy slope are two criteria to identify the POCs originating from the cooling of GRB electrons. Because the spectral criterion is only an inequality, that criterion is rather weak and could yield many "false positives", as POC arising from other mechanisms may satisfy it.

Figure 1 and Table 4 show that most OFs, defined by $\beta_{o\gamma} < \beta_{LE}$ (i.e. POCs that are brighter than expected from the cooling of GRB electrons in a constant magnetic field), do not satisfy the temporal correlation expected for POCs from electron cooling ($\delta t_o \simeq \delta t_\gamma$ for POCs, $\Delta t_o \simeq \delta t_o$ for delayed OCs).

We note that an increasing magnetic field could account for the higher brightness of OFs even when they arise from the cooling of GRB electrons, and that such an increasing magnetic field should not invalidate the expected temporal correlations for each POC type because those correlations arise from that the electron cooling-time at energy ϵ is comparable to the electron transit-time to energy ϵ , which is correct even for a variable B .

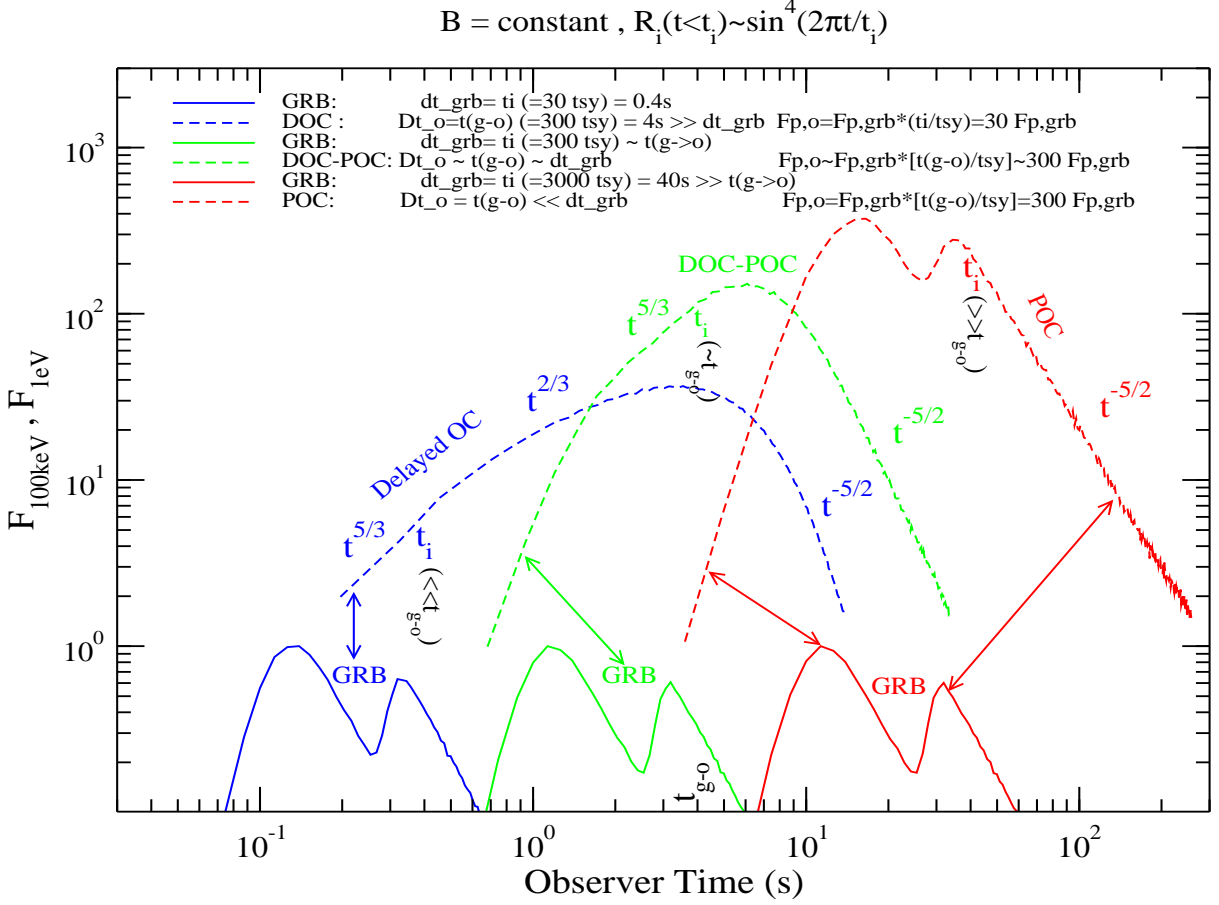


FIG. 2.— Metamorphosis of a delayed optical counterpart (DOC) into a (truly) prompt optical counterpart (POC) obtained by increasing the duration t_I of electron injection (which sets the duration δt_γ of the GRB pulse), from well-below to well-above the GRB-to-optical transit time $t_{\gamma o} = 300 t_{\text{sy},i}$ (which sets the GRB-to-optical peak time-delay Δt_o). Parameters are: magnetic field $B = 100$ G, electrons are injected above energy $\gamma_i = 3 \times 10^4$, with a $p = 3$ power-law distribution with energy, source Lorentz factor $\Gamma = 100$. The peak energy of the $\epsilon \mathcal{F}_\epsilon$ spectrum is $E_\gamma \simeq 200$ keV, the observer-frame SY cooling-time is $t_{\text{sy},i}^{(\text{obs})} = t_{\text{sy},i}/(2\Gamma) = 13$ ms and the GRB-to-optical transit-time $t_{\gamma o} = 4\text{s}$. The GRB peak flux normalized at unity (but 1 mJy is a typical/average peak flux). The electron injection has with two sinusoidal pulses and the electron cooling is SY dominated. For $t_I \gg t_{\text{sy},i}$, the GRB pulse has two peaks at $t_I/4$ and $3t_I/4$ (slightly delayed by the angular integration) and the optical pulse peaks are delayed by $t_{\gamma o}$. The legend quantifies the optical-to-GRB peak flux-ratio and the relationship between δt_γ and Δt_o , with GRB and optical pulses of same t_I being shown with the same color. That $\delta t_\gamma = t_I$ and $\Delta t_o = t_{\gamma o}$ imply that: *i*) a DOC (blue), defined by $\delta t_\gamma < \Delta t_o$, is obtained for $t_I \ll t_{\gamma o}$ (peak-flux ratio on middle line of eq (24) in PV22, *ii*) an intermediate DOC-POC (green), defined by $\delta t_\gamma \simeq \Delta t_o$, results for $t_I \simeq t_{\gamma o}$, and *iii*) a POC (red), defined by $\Delta t_o \ll \delta t_\gamma$, occurs for $t_I \gg t_{\gamma o}$, with the peak-flux ratio reaching maximal value (last case in eq (24) of PV22). The variability timescale $t_I/2$ of the sinusoidal electron injection rate R_i that is displayed by the GRB flux appears also in the optical if the GRB-to-optical transit time $t_{\gamma o}$ is shorter than the injection variability timescale $t_I/2$, which means that the GRB variability is preserved for POCs (because $\Delta t_o \sim t_{\gamma o}$, $t_I \sim \delta t_\gamma$ and $t_{\gamma o} < t_I/2$ imply $\Delta t_o < \delta t_\gamma$). For $t_I \ll t_{\gamma o}$, the two sines of injected electrons cool and reach optical-emitting energies separated by $t_I/2 \ll t_{\gamma o} \simeq \Delta t_o$, with integration over the synchrotron function and the angular opening of the ejecta ironing out the initial variability, which means that GRB variability is lost for DOCs (similar to above, $t_I < t_{\gamma o}$ implies $\delta t_\gamma < \Delta t_o$). Thus, *delayed OCs lose the GRB variability, but prompt OCs retain it*. The indicated OC flux power-laws are those of eq (21) in PV22 : $f_\epsilon(t < t_I/2) \sim t^{5/3}$, $f_\epsilon(t_I/2 < t < t_{\gamma o}) \sim t^{2/3}$ with $t_I/2$ marking the end of the first injection episode, and are close to those displayed by the rise of the OC flux calculated numerically despite that the first analytical result (for $t < t_I/2$) was derived for a constant injection rate. (The $f_\epsilon \sim t^4$ earliest rise shows the injection rate R_i , the emission from the cooling tail being overshadowed by the sharp rise of R_i). The OC power-law falling flux is the LAE given in eq (26) of PV22 for the slope $\beta = -1/2$ of the integrated spectrum of the SY emission from a quasi-monoenergetic cooled electron distribution.

This implies that the temporal criterion for the identification of POCs from the cooling of GRB electrons works even for a variable magnetic field, while the spectral criterion is useful only for a constant magnetic and may miss true POCs from GRB electron cooling if the magnetic field is increasing.

Thus, the temporal criterion is clearly superior to the spectral one in selecting POCs that arise from the cooling of GRB electrons, but that does not mean that the spectral criterion is useless because the temporal criterion has a limitation that is alleviated by adding the spectral criterion. Because the temporal correlations induced by electron cooling arise solely from the pulse peak-epoch being comparable to the pulse duration ($t_p^{(\epsilon)} \simeq \delta t_\epsilon$), it is not sensitive to the origin of the cooling electrons and cannot discriminate among various mechanisms that produce optical emission (pairs produced by GeV photons, reverse-shock, SY emission in synchrotron self-Compton GRBs) if the timing of POC pulse is set by cooling of electrons.

If the POC arises from another mechanism overshadowing the emission from cooling GRB electrons, then the POC will not satisfy the spectral condition $\beta_{o\gamma} > \beta_{LE}$. Consequently, adding the spectral condition to the temporal criterion is a trade-off, as it increases the probability that an POC satisfying both criteria arises from the cooling of GRB electrons, at the risk of missing some true POCs from GRB electrons cooling in an increasing magnetic field.

Putting together the considerations in §4.1, one can conclude that *GRB variability is passed on the OC only for POCs*, with that being either an observational bias (for GRB variability arising from fluctuations in the magnetic field) or a consequence of electron cooling (for GRB variability from fluctuations in the injection rate). To the extent that OC variability can be measured by robotic telescopes, this conclusion provides another criterion for identifying OCs arising from the cooling of GRB electrons.

5. CONCLUSIONS

The aim of this work is to investigate what new information can be extracted from the properties of the Prompt Optical Counterparts resulting from cooling of GRB electrons.

Starting from the durations δt_γ and δt_o of GRB and POC pulses (which are set by the corresponding electron cooling times for the emission from a bright-spot, the angular time-spread t_{ang} for the emission from a uniform-brightness surface or for AD-cooling, or the two temporal

parameters t_B and t_I for the duration of magnetic field and electron injection) and the lag-time Δt_o between the peaks of the GRB and POC pulses (which is set by the gamma-to-optical transit-time $t_{\gamma o}$ or by the timescale t_B), it can be shown that the POCs arising from the cooling of GRB electrons are of two types: "prompt", for which $\Delta t_o < \delta t_\gamma = \delta t_o$, and "delayed", for which $\delta t_\gamma < \Delta t_o = \delta t_o$.

The preceding inequalities are definitions and the following equalities represent a test for the electron-cooling model for POCs. Adding the condition $\beta_{o\gamma} \geq \beta_{LE}$ between the POC-to-GRB effective spectral slope $\beta_{o\gamma}$ and the GRB low-energy slope β_{LE} strengthens this temporal criterion for identifying POCs arising from the cooling of GRB electrons by discriminating the POCs arising from other mechanisms (involving electron cooling or not), although that may miss some POCs from cooling if GRB electrons if the magnetic field were to increase.

Adding that POCs should be associated more often with GRBs with a harder low-energy slope β_{LE} , these two correlations imply that POCs should be dimmer (on average) than delayed ones. This correlation finds support in a set of ten POCs, with the average POC-to-GRB brightness ratio $\beta_{o\gamma}$ being harder for POCs.

If GRB electrons that do not cool significantly during the magnetic field life then the burst should have a hard low-energy slope $\beta_{LE} = 1/3$ and the POC should be prompt and dimmer be a factor $(100keV/1keV)^{1/3}$ (about 4 magnitudes) than the burst. Thus, a burst of average flux of 1 (10) mJy will be accompanied by an POC of magnitude $R = 20$ (18), which implies that some GRBs with a hard low-energy slope β_{LE} will be accompanied by a prompt and dim intrinsic POC emission (from cooling of GRB electrons) that is difficult to detect with robotic telescopes. That sets a bias against detecting the intrinsic POCs of hard GRBs.

If GRB electrons cool to optical energies then the burst should have a soft low-energy slope $\beta_{LE} = -1/2$ (for SY-dominated electron cooling) and the POC may be brighter than the burst by a factor up to $(100keV/1keV)^{1/2}$ (6 magnitudes). Thus, the POC of a burst with a soft slope β_{LE} and average flux of 1 (10) mJy could be as bright as magnitude $R = 10$ (7.5), which is comparable to the brightness of the OFs accompanying GRBs 990123, 080319B, and 130427A (Table 4). However, all those bursts have a hard low-energy slope $\beta_{LE} > 0$, which implies an incomplete electron cooling and yields a dim intrinsic POC emission (from the cooled GRB electrons), thus their OFs must have arose from another mechanism (emission from pairs formed from the GeV prompt emission, external reverse-shock, SY emission in the synchrotron self-Compton model for GRBs).

REFERENCES

- Abdo A. et al, 2009, Science 323, 688
 Ackermann M. et al, 2014, Science 343, 42
 Akerlof C. et al, 1999, Nature 389, 400
 Blake C. et al, 2005, Nature 435, 181
 Corsi A. et al, 2005, A&A 438, 829
 Cucchiara A. et al, 2011, ApJ 743, 154
 Elliott J. et al, 2014, A&A 562, 100
 Gendre B. et al, 2012, ApJ 748, 59
 Greiner J. et al, 2014, A&A 568, 75
 Gruber D. et al, 2011, A&A 52, 15
 Karpov S. et al, 2017, ASPC 510, 309
 Klotz A. et al, 2008, A&A 483, 847
 Kopac D. et al, 2013, ApJ 772, 73
 Kumar P. et al, 2007, MNRAS 376, L57

- Martin-Carillo A. et al, 2014, A&A 567, 84
Mészáros P., Rees M., 1997, ApJ 476, 232
Mészáros P., Rees M., 1999, MNRAS 306, L39
Page K. et al, 2007, ApJ 663, 1125
Panaitescu A., Mészáros P., 1998, ApJ 492, 683
Panaitescu A., Kumar P., 2007, MNRAS 376, 1065
Panaitescu A., 2015, ApJ 806, 64
Panaitescu A., Vestrand W., 2022, ApJ, accepted,
arXiv:2209.10014 (PV22)
Papathanassiou H., Mészáros P., 1996, ApJ 471, L91
Racusin J. et al, 2008, Nature 455, 183
Ravasio M. et al, 2018, A&A 613, 16
Sari R., Piran T., 1999, ApJ 517, L109
Stratta G. et al, 2013, ApJ 779, 66
Thone C. et al, 2010, A&A 523, 70
Vestrand W. et al, 2005, Nature 435, 178
Vestrand W. et al, 2006, Nature 442, 172
Vestrand W. et al, 2014, Science 343, 38
Virgili F. et al, 2013, ApJ 778, 54
Vurm I., Hascoet R., Beloborodov A., 2014, ApJ 789, L37
Wozniak P. et al, 2009, ApJ 691, 495